Int J Clin Exp Med 2020;13(10):7622-7629
www.ijcem.com /ISSN:1940-5901/IJCEM0112634

Original Article

Effects of small RNA interference-mediated silencing of S100A13 on invasion and migration of thyroid cancer cell line TPC-1

Jialiang Xing[1], Ning Cao[2], Xiaolin Pan[2], Mingwen Yu[1], Nana Xu[1], Ke Han[1]

[1]General Surgery, The 5th People's Hospital of Ji'nan, Ji'nan, Shandong, China; [2]General Surgery, Jinan Seventh People's Hospital, Ji'nan, Shandong, China

Received April 15, 2020; Accepted June 23, 2020; Epub October 15, 2020; Published October 30, 2020

Abstract: Aim: To investigate the effect and mechanism of small RNA interference-mediated silencing of S100A13 (S100 Calcium Binding Protein A13) on the invasion and migration of thyroid cancer cell line TPC-1. Methods: The S100A13 gene in TPC-1 cells was knocked down by small RNA. The effect of S100A13 knockdown on the migration ability of TPC-1 cells was tested by Transwell and cell scratch assays, and the expression of Vimentin (Vimentin), E-cadherin (Cadherin E protein), and MMP-2 (matrix metalloproteinase 2) were all determined by Western blot. Results: Compared with the blank and the negative control groups, the siRNA-A13 group exhibited lower expression level of S100A13 protein, OD values, absorbance, higher expression of E-cadherin/GAPDH, and lower expression of Vimentin/GAPDH and MMP-2/GAPDH ($P<0.05$). Conclusion: S100A13 silencing can inhibit the invasion and migration of TPC-1 cells, which may be related to promotion of E-cadherin expression and inhibition of MMP-2 and Vimentin expression in TPC-1 cells.

Keywords: Small RNA, interference, silencing, thyroid cancer cell, invasion, migration

Introduction

Thyroid cancer is the most common malignant tumor of the endocrine system. The early signs of thyroid cancer are very subtle, and its severity also varies from person to person [1]. For this reason, it is necessary to find a highly sensitive genetic diagnostic method to confirm the diagnosis early, which could improve the prognosis of patients with thyroid cancer, [2]. Clinical studies have shown that patients with thyroid cancer have deletions or point mutations in tumor suppressor genes, and overexpression of oncogenes. Previous studies mainly centered on the already recognized Bcl-2, gsp, c-myc, NTRK1, Ras, Ret/PTC oncogenes and tumor suppressor genes such as nm23, P16, Rb, and P53, because tumorigenesis is a pathological processes involving multiple factors and genes [3, 4]. In addition to the above genes, there are other genes worth investigating in thyroid cancer [5].

The invasion and migration of thyroid cancer cells is a complex process. The reduction of the cellular matrix, intercellular adhesion, and extracellular matrix degradation could impact thyroid tissue metastasis [6, 7]. The S100 protein family is composed of 21 members that exhibit a high degree of structural similarity, which is closely related to pathological processes such as tissue damage and repair, tumors, and inflammation, and has drawn much clinical attention in recent years [8]. S100A13 is a new member of this family. Its biological functions, structure, subcellular localization, and tissue distribution are different from other proteins in the S100 family; suggesting that S100A13 has unique biological activity not found in the S100 family [9, 10]. Studies have shown that S100A13 can be expressed in various tissues, and can migrate across the membrane of cytokines, and play an important part in the development of atherosclerosis, the inflammatory response, and tumors [11].

Clinical studies have shown that the expression of S100A13 in thyroid cancer tissues is significantly increased, but the specific mechanism of S100A13 in the migration and invasion of these tumors has not been fully explored [12]. This study aimed to investigate the effect of small RNA interference-mediated silencing of S100A13 on the invasion and migration of TPC-1 cells.

Materials and methods

Instruments and reagents

Human thyroid cancer cell line TPC-1 (Cell Bank of the Chinese Academy of Sciences); MMP-2 antibody, vimentin antibody, and cadherin E antibody (Cellular Technology Ltd. US); ECL liquid, BCA protein quantification kit, PVDE (Millipore); USA; 5 × SDS Loading buffer, RIPA/PMSF cell lysate, Transwell chamber (Beijing Solibao Technology Co., Ltd.); Goat anti-mouse IgG, HRP, GAPDH antibody (Beijing Zhongshan Jinqiao Co., Ltd.); Matrigel (BD, US); Lipofectamine 2000 (Invitrogen); 0.25% Trypsin, PBS, fetal bovine serum, RPMI-1640 culture solution (Hyclone); Enzyme-linked immunoassay instrument (Molecular Devices); protein electrophoresis tank (Bio-Rad); Benchtop Centrifuge (Molecular Devices); Inverted microscope (Leica, Germany); Cell incubator (Sanyo, Japan); Biological safety cabinet (Haier).

Cell culture

Human thyroid cancer cell line TPC-1 was cultured in RPMI-1640 medium (containing 10% fetal bovine serum) and placed inside a 37°C cell incubator with saturated humidity. The medium was replaced every 24 h. Next, 0.25% Trypsin was added at 90% cell confluence, and the passage ratio was controlled at 1:3 or 1:2.

Cell transfection

Twenty-four hours before transfection, 2.5-3.0 × 10^5 cells were seeded per well in 6-well plates. When the cell density reached 80%-90% confluence, cells were divided into the: siRNA-A13 group (siRNA G), negative control group (NCG) and blank control group (BCG) for transfection. Then, 5 μl of siRNA was added to 250 μl of culture medium (serum-free), mixed uniformly, and was allowed to stand for 5 minutes. Next, 5 μl of Lipo 2000 was added to 250 μl of culture medium (serum-free), and was allowed to stand for 5 minutes. The above two solutions were mixed uniformly, and kept at room temperature for 10-20 min. We then, remove the culture solution and washed 3 times with PBS and added serum-free culture solution. The lipid complex was added to the 6-well plate, the volume of each well was kept at 2 ml, stored in the dark, at 37°C. After 6 h of incubation in a 5%, CO_2 incubator, it was replaced with a complete culture solution and cultured for 48 h. The transfection was determined by immunoblotting test.

Cell scratch assay

Cells were given 10% fetal bovine serum, and seeded in a 6-well plate with 3 × 10^5 cells/well. When the cell density reached 90% confluence, the cell layer was scratched vertically using a sterile pipet tip. The cells were washed with serum-free medium, and cultured in a 5%, 37°C, CO_2 incubator for 24 hours. Then the average cell scratch healing distance was observed with Image J software, and the scratch width was calculated.

Cell migration

The cell density was adjusted to (3.0-4.0) × 10^5 cells per well. The Transwell chamber was placed in a 24-well plate. Next, 200 μl of cell suspension was added to the upper chamber while 600 μl RPMI-1640 containing bovine serum was added to the lower chamber, followed by incubation at 5% CO_2 and 37°C for 24 hours. The chamber was removed, the culture solution was aspirated off, and the remaining cells in the microporous membrane were carefully wiped off with a cotton swab and washed with PBS solution that was fixed with methanol for 30 min, followed by crystal violet staining under the assistance of a 400 × light microscope. The experiment was repeated 3 times, and 10% acetic acid was used for elution treatment. Cell absorbance was read with a microplate reader.

Cell invasion

Serum-free RPMI-1640 medium was diluted 1:1 with Matrigel 50 mg/L and incubated at 37°C for 60 min. Serum-free medium was added to each well before the experiment, and incubated at 37°C for 30 min. Transwell chambers were loaded on a 24-well plate. Next, 600

Table 1. Effect of small RNA on the expression of S100A13 protein in TPC-1 cells ($\bar{x}\pm s$)

Group	S100A13 protein
siRNA-A13	0.273±0.021
Negative control	0.540±0.052*
Blank control	0.526±0.059*
F	52.632
P	0.000

Note: *indicates comparison with siRNA-A13 group, *P*<0.05.

μl of RPMI-1640 culture solution (containing 10% fetal bovine serum) was added to the lower chamber, while 1 × 10^5 cells from each group were add to the upper chamber, followed by incubation at 37°C for 24 hours. The remaining cells are wiped off with cotton swabs, and treated with 1% crystal violet stain for 15-20 min under a 400 × light microscope in different 10 fields of view. The experiment was repeated 3 times. After elution with 10% acetic acid, absorbance of the cells was determined by a microplate reader.

Vimentin, E-cadherin, MMP-2 expression assays

Western blot was used to measure the expression of Vimentin, E-cadherin and MMP-2. The specific methods were as follows: The culture medium was removed and washed with PBS solution 3 times. Then, 80 μl of RIPA lysate was added into each cell in the 6-well plate, and the cells were transferred to the centrifuge tube and placed on ice. Vortex oscillation was performed once every 5 min to ensure sufficient cell lysis. The cell suspension was collected and centrifuged to obtain the supernatant. The separation gel was set in strict accordance with the molecular weight of the sample to be tested, and it was rapidly perfused in the gap between the glass plates. At the same time, 1 ml of anhydrous ethanol was filled in and the liquid was sealed. After the separation gel polymerization was observed, anhydrous ethanol was removed. The concentrated gel was prepared and the perfusion process was completed. The comb was inserted and left standing for 30 min at room temperature, and then fixed on the electrophoresis device. The 5 × SDS Loading buffer (4:1) was fully mixed with the protein sample and boiled for 5-10 min. Wells of gel sample were washed with electrophoretic buffer, and the equal volume of denatured protein was added. Electrophoresis (70 V) was performed for 1 h until the blue bands were separated. The voltage was controlled at 100-110 V. The electrophoresis was stopped when the bromophenol blue reached the bottom of the separation gel. The sponge pad, PVDF membrane and filter paper were soaked in the transfer buffer for 5 min. The transfer device was assembled with the current adjusted to 250 mA during the ice bath, and the membrane was transferred for 1.5-2.5 h. The membrane was placed in 5% blocking solution and incubated at room temperature for 1.5-3 h, which was rinsed 3 times with TBST solution for 5-10 min each. The primary antibody was added and incubated at 4°C overnight. It was rinsed 3 times with 0.1% TBST solution for 10 min each time. The secondary antibody was added and incubated at room temperature for 1 h, and then washed 3 times with 0.1% TBST for 10 min each. ECL was performed, and the gray value of the protein was analyzed by Image J software.

Outcome measurements

(1) The effect of small RNA on the expression of S100A13 protein in TPC-1 cells.

(2) Effects of S100A13 silencing on the migration ability of TPC-1 cells.

(3) Effects of S100A13 silencing on the invasion ability of TPC-1 cells.

(4) The effect of S100A13 silencing on the expression of Vimentin, E-cadherin and MMP-2.

Statistical methods

SPSS 22.0 was used for analysis. Means± standard deviation were used to represent the measurement data. Data that met a normal distribution were subjected to the t-test. If not, the Mann-Whitney U test was used. Comparison of count data was performed by chi-aquared test, P<0.05 was deemed as statistically significant.

Results

Effect of small RNA on the expression of S100A13 protein in TPC-1 cells

According to Western Blot results, the expression of S100A13 protein in the siRNA G was (0.273±0.021); the NCG was (0.540±0.052),

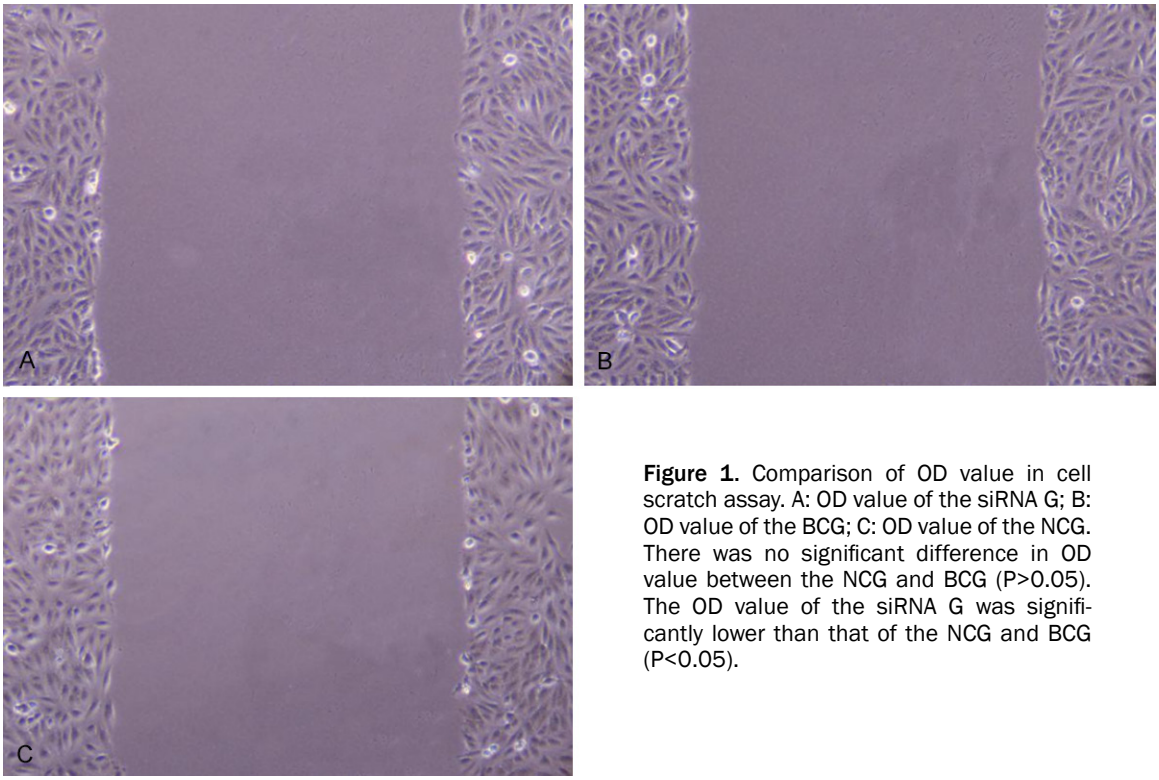

Figure 1. Comparison of OD value in cell scratch assay. A: OD value of the siRNA G; B: OD value of the BCG; C: OD value of the NCG. There was no significant difference in OD value between the NCG and BCG (P>0.05). The OD value of the siRNA G was significantly lower than that of the NCG and BCG (P<0.05).

Table 2. Inhibition of migration ability of TPC-1 cells by silenced S100A13 ($\bar{x}$±s)

Group	Scratch width (mm)	OD
siRNA-A13	69.238±5.125	0.762±0.062
Negative control	29.865±3.122*	1.205±0.111*
Blank control	25.212±2.128*	1.258±0.113*
F	25.965	63.259
P	0.000	0.000

Note: *indicates comparison with siRNA-A13 group, *P*<0.05.

and the BCG was (0.526±0.059). However, the expression of S100A13 protein in the siRNA G was lower than in controls (P<0.05) (**Table 1**; **Figure 1**).

Effects of S100A13 silencing on the migration ability of TPC-1 cells

The scratch width of the siRNA G was (69.238±5.125) mm; the NCG was (29.865±3.122) mm, and the BCG was (25.212±2.128) mm. Compared with the BCG and the NCG, the scratch width of the siRNA G was significantly wider (P<0.05), The OD value of the siRNA G was (0.762±0.062) mm, the NCG was (1.205±0.111) mm, and the BCG was (1.258±0.113) mm. Compared with the blank and NCGs, the OD value of the siRNA G was lower (P<0.05) (**Table 2**; **Figure 2**).

Effects of S100A13 silencing on the invasion ability of TPC-1 cells

The absorbance of the siRNA G was (0.522±0.025), the NCG was (0.932±0.012), and the BCG was (0.912±0.015).

The NCG and the BCG did not differ in absorbance (P>0.05). Compared with these two groups, the absorbance of the siRNA G was lower (P<0.05, **Table 3**; **Figure 3**).

Effect of S100A13 silencing on Vimentin, E-cadherin, MMP-2 levels

Compared with control groups, siRNA G exhibited higher expression of E-cadherin/GAPDH and lower level of Vimentin/GAPDH, MMP-2/GAPDH (P<0.05) (**Table 4**; **Figure 4**).

Discussion

S100 protein family of calcium binding proteins exhibit similar spatial structures and can interact with calcium ions [13, 14]. S100 protein

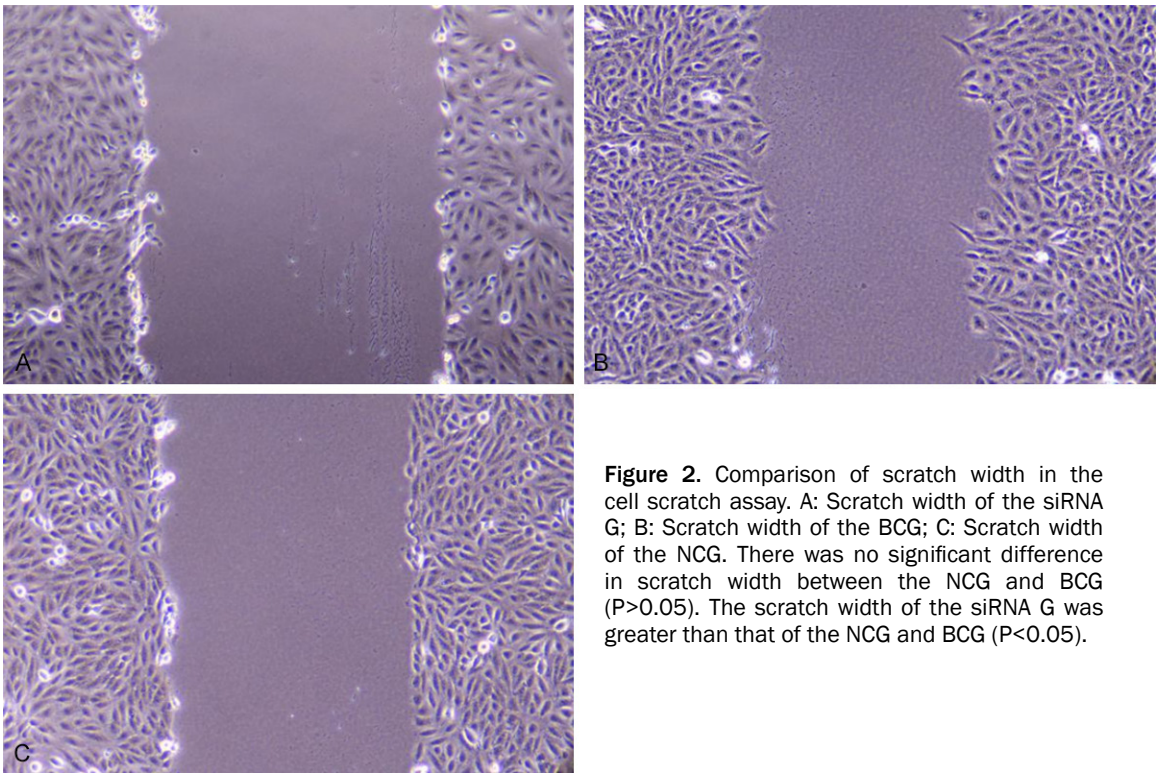

Figure 2. Comparison of scratch width in the cell scratch assay. A: Scratch width of the siRNA G; B: Scratch width of the BCG; C: Scratch width of the NCG. There was no significant difference in scratch width between the NCG and BCG (P>0.05). The scratch width of the siRNA G was greater than that of the NCG and BCG (P<0.05).

Table 3. Inhibition of invasion ability of TPC-1 cells by silenced S100A13 ($\bar{x}$±s)

Group	Absorbance
siRNA-A13	0.522±0.025
Negative control	0.932±0.012*
Blank control	0.912±0.015*
F	28.858
P	0.000

Note: *indicates comparison with siRNA-A13 group, P<0.05.

shows specific tissue and cell distribution and is closely related to pathophysiological processes such as tissue damage repair, tumors and inflammation; which is a hot topic in clinical research [15]. The S100A13 gene is located on human chromosome 1q21, and the entire length of DNA is 8979 bp [16]. The chromosomal location of the S100A13 gene is between the S100A13 and S100A1 genes, and together with the S100A16 gene, S100A14 gene, and the S100A1 gene; they form a gene subgroup [17]. Studies have shown that the S100A13 gene is highly expressed in the thymus, thyroid, bladder, small intestine, uterus, pancreas, kidney, heart muscle, skeletal muscle, brain tissues and other organs; and lowly expressed in the stomach, prostate, and liver: indicating that the S100A13 gene has a role in various pathophysiological processes [18, 19].

In this study, the siRNA G had lower protein expression level and OD value of S100A13, larger scratch width, and lower absorbance compared with the BCG and the NCG (P<0.05), indicating that S100A13 silencing can inhibit the migration and invasion of TPC-1 cells. Clinical studies have shown that the invasion ability of lung cancer cells largely depended on the expression level of S100A13, which is similar to the findings of this study. The expression level of the S100A13 gene in thyroid cancer tissue is significantly increased. siRNA can inhibit the carcinogenicity of thyroid cancer AW579 and TPC-1 by knocking out the S100A13 gene. This suggests that S100A13 could be used as an important biomarker for the diagnosis of thyroid cancer in clinic, but its specific mechanism of action has not been fully clarified [20].

The epithelial-mesenchymal transition (EMT) plays a role in the invasion and migration of tumor cells and embryonic development [21]. During this process, the cell migration ability is enhanced, but its adhesion ability is decreased, and the cell phenotype is also changed. During

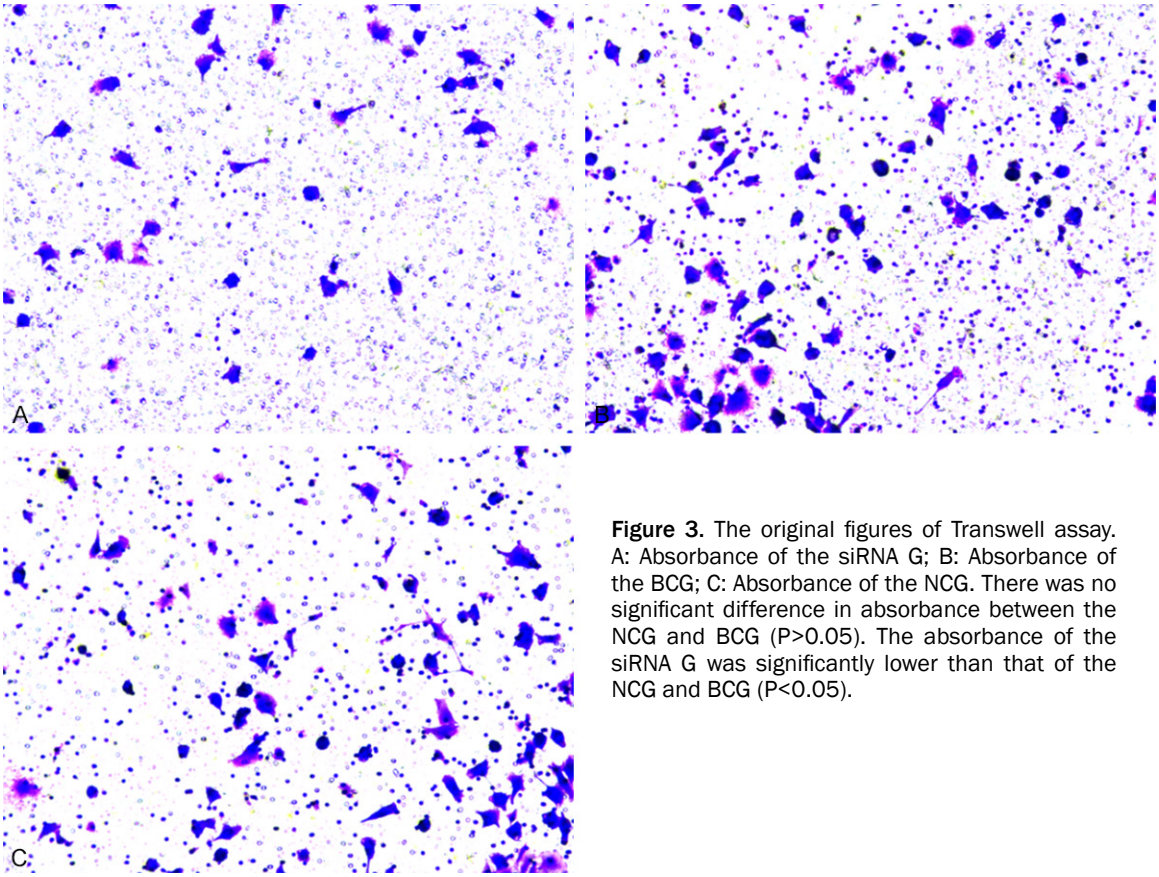

Figure 3. The original figures of Transwell assay. A: Absorbance of the siRNA G; B: Absorbance of the BCG; C: Absorbance of the NCG. There was no significant difference in absorbance between the NCG and BCG ($P>0.05$). The absorbance of the siRNA G was significantly lower than that of the NCG and BCG ($P<0.05$).

this process, the unique properties of mesenchymal cells will gradually emerge, and the ability of cell migration and invasion will be significantly improved. Therefore, the appearance of EMT could be regarded as an early sign of tumor cell metastasis and invasion [22, 23]. Intermediate filament protein is one of the important markers of interstitial cells, which is activated by vimentin on the cytoskeleton. The change of its expression level could indicate the occurrence of EMT [5]. Similarly, when the expression of E-cadherin was reduced, it also indicated the occurrence of EMT, so this is also used as an important marker for the occurrence of EMT in clinical practice. Clinical studies have shown that changes in the expression level of multiple genes can inhibit or promote the EMT process to varying degrees during the development of thyroid cancer [24]. When epithelial cells are transformed into mesenchymal cells, the intercellular adhesion and connectivity will disappear, the cell migration and invasion ability will be significantly improved, and a large number of extracellular matrix components will also be produced [25]. MMP-2 is closely correlated with extracellular matrix degradation, which in turn promotes tumor cell invasion and migration.

In this study, compared with the BCG and NCG, the siRNA G had higher levels of E-cadherin/GAPDH and lower levels of Vimentin/GAPDH and MMP-2/GAPDH ($P<0.05$). The mechanism of decreased expression of silencing S100A13 may be attributed to the following: S100A13 silencing can inhibit the invasion and migration of TPC-1 cells via promoted expression of E-cadherin and inhibited expression of MMP-2 and Vimentin, which blocks EMT process and the extracellular matrix of thyroid cancer cells. However, the study also has some limitations. Further research is needed to investigate the underlying mechanism with regard to the effects of S100A13 silencing by small RNA on cell invasion and migration.

In summary, silencing S100A13 expression with small RNA can inhibit the invasion and migration of TPC-1 cells, which may be related to the promotion of E-cadherin expression and

Table 4. Effect of Silencing S100A13 on Vimentin, E-cadherin, MMP-2 Expression ($\bar{x}$±s)

Group	MMP-2/GAPDH	E-cadherin/GAPDH	Vimentin/GAPDH
siRNA-A13	0.248±0.023	0.758±0.012	0.421±0.052
Negative control	0.543±0.026*	0.456±0.048*	0.859±0.058*
Blank control	0.522±0.026*	0.448±0.042*	0.865±0.038*
F	18.963	28.788	35.698
P	0.000	0.000	0.000

Note: *indicates comparison with siRNA-A13 group, P<0.05.

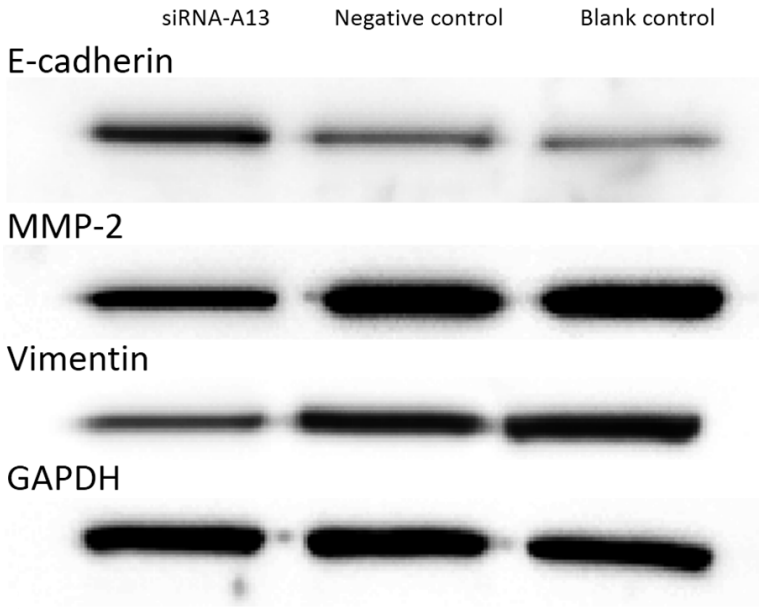

Figure 4. The original figures of Western blot. There was no significant difference in MMP-2/GAPDH, E-cadherin/GAPDH, and Vimentin/GAPDH between the NCG and the BCG (P>0.05). siRNA G had higher E-cadherin/GAPDH and lower Vimentin/GAPDH and MMP-2/GAPDH compared with the NCG and the BCG (P<0.05).

inhibition of MMP-2, as well as Vimentin expression in TPC-1 cells.

Disclosure of conflict of interest

None.

Address correspondence to: Ke Han, General Surgery, The 5th People's Hospital of Ji'nan, No.24297, Jingshi Road, Ji'nan 250101, Shandong, China. Tel: +86-150-9890-8805; E-mail: hankeee1@163.com

References

[1] Kitagawa Y, Tsurui M and Hasegawa Y. Steric and electronic control of chiral Eu(III) complexes for effective circularly polarized luminescence. ACS Omega 2020; 5: 3786-3791.

[2] M'Hamedi A and Batsanov AS. Phospho-rescent mono- and diiridium(III) complexes cyclo-metalated by fluorenyl- or phenyl-pyridino ligands with bulky substituents, as prospective OLED dopants. Acta Crystallogr E Crystallogr Commun 2020; 76: 392-399.

[3] Monteiro DCF, von Stetten D, Stohrer C, Sans M, Pearson AR, Santoni G, van der Linden P and Trebbin M. 3D-MiXD: 3D-printed X-ray-compatible microfluidic devices for rapid, low-consumption serial synchrotron crystallography data collection in flow. IUCrJ 2020; 7: 207-219.

[4] Sikri G and Sawhney RS. First principle approach to elucidate transport properties through L-glutamic acid-based molecular devices using symmetrical electrodes. J Mol Model 2020; 26: 74.

[5] Veličković D, Zhang G, Bezbradica D, Bhattacharjee A, Paša-Tolić L, Sharma K, Alexandrov T and Anderton CR. Response surface methodology as a new approach for finding optimal MALDI Matrix spraying parameters for mass spectrometry imaging. J Am Soc Mass Spectrom 2020; 31: 508-516.

[6] Feng H, Magda JJ and Gale BK. Viscoelastic second normal stress difference dominated multiple-stream particle focusing in microfluidic channels. Appl Phys Lett 2019; 115: 263702.

[7] Smidt TE, Mack SA, Reyes-Lillo SE, Jain A and Neaton JB. An automatically curated first-principles database of ferroelectrics. Sci Data 2020; 7: 72.

[8] Zhou J, Chizhik AI, Chu S and Jin D. Single-particle spectroscopy for functional nanomaterials. Nature 2020; 579: 41-50.

[9] Su Y, Xu C, Sun Z, Liang Y, Li G, Tong T and Chen J. S100A13 promotes senescence-associated secretory phenotype and cellular senescence via modulation of non-classical secretion of IL-1α. Aging (Albany NY) 2019; 11: 549-572.

[10] Bai Y, Li LD, Li J and Lu X. Prognostic values of S100 family members in ovarian cancer patients. BMC Cancer 2018; 18: 1256.
[11] Miao S, Qiu T, Zhao Y, Wang H, Sun X, Wang Y, Xuan Y, Qin Y and Jiao W. Overexpression of S100A13 protein is associated with tumor angiogenesis and poor survival in patients with early-stage non-small cell lung cancer. Thorac Cancer 2018; 9: 1136-1144.
[12] Cheng G, Chung PH, Chan EK, So MT, Sham PC, Cherny SS, Tam PK and Garcia-Barceló MM. Patient complexity and genotype-phenotype correlations in biliary atresia: a cross-sectional analysis. BMC Med Genomics 2017; 10: 22.
[13] Inoue O, Hokamura K, Shirai T, Osada M, Tsukiji N, Hatakeyama K, Umemura K, Asada Y, Suzuki-Inoue K and Ozaki Y. Vascular smooth muscle cells stimulate platelets and facilitate thrombus formation through platelet CLEC-2: Implications in Atherothrombosis. PLoS One 2015; 10: e0139357.
[14] Ite K, Yonezawa K, Kitanishi K, Shimizu N and Unno M. Optimal mutant model of human S100A3 protein citrullinated at Arg51 by peptidylarginine deiminase type III and its solution structural properties. ACS Omega 2020; 5: 4032-4042.
[15] Jung YH, Han D, Shin SH, Kim EK and Kim HS. Proteomic identification of early urinary-biomarkers of acute kidney injury in preterm infants. Sci Rep 2020; 10: 4057.
[16] Sidorin VS, Zabrodskaya YM and Dobrogorskaya LN. Tanatogenetic role of type 2 diabetes in neurosurgical patients. Arkh Patol 2020; 82: 38-46.
[17] Sun H, Zhao A, Li M, Dong H, Sun Y, Zhang X, Zhu Q, Bukhari AA, Cao C, Su D, Liu Y and Liang X. Interaction of calcium binding protein S100A16 with myosin-9 promotes cytoskeleton reorganization in renal tubulointerstitial fibrosis. Cell Death Dis 2020; 11: 146.
[18] Gonzalez LL, Garrie K and Turner MD. Role of S100 proteins in health and disease. Biochim Biophys Acta Mol Cell Res 2020; 1867: 118677.
[19] Madda R, Chen CM, Wang JY, Chen CF, Chao KY, Yang YM, Wu HY, Chen WM and Wu PK. Proteomic profiling and identification of significant markers from high-grade osteosarcoma after cryotherapy and irradiation. Sci Rep 2020; 10: 2105.
[20] Jiang P and Lai J. Merkel cell carcinoma clinically mimicking a traumatic suture scar in the nasal vestibule: earlier diagnosis for better prognosis. Anticancer Res 2020; 40: 1123-1126.
[21] Hu CX, Hu KY and Wang JF. Potential role of the compound Eucommia bone tonic granules in patients with osteoarthritis and osteonecrosis: a retrospective study. World J Clin Cases 2020; 8: 46-53.
[22] Gross J and Fritchie K. Soft tissue special issue: biphenotypic sinonasal sarcoma: a review with emphasis on differential diagnosis. Head Neck Pathol 2020; 14: 33-42.
[23] Li C, Ma Y, Fei F, Zheng M, Li Z, Zhao Q, Du J, Liu K, Lu R and Zhang S. Critical role and its underlying molecular events of the plasminogen receptor, S100A10 in malignant tumor and non-tumor diseases. J Cancer 2020; 11: 826-836.
[24] Ungari M, Trombatore M, Ferrero G, Gusolfino MD, Manotti L, Tanzi G, Varotti E and Bertoni R. Eosinophilic cytoplasmic inclusions in type 2 papillary renal cell carcinoma. Pathologica 2019; 111: 369-374.
[25] Mondet J, Laurin D, Lo Presti C, Jacob MC, Meunier M, Giraudon E, Lefebvre C, Berthier S, Leer AM, Park S and Mossuz P. Increased S100A8 expression in bone marrow plasma by monocytic cells from acute myeloid leukemia patients. Hematol Oncol 2020; 38: 114-118.